COMPARING FILTERS FOR CORRECTION OF SECOND ORDER DIFFRACTION EFFECTS IN HYPERSPECTRAL IMAGERS

Marie Bøe Henriksen[1,2]*, Fred Sigernes*[1,2] *and Tor Arne Johansen*[1]

[1] Norwegian University of Science and Technology (NTNU), Trondheim, Norway
[2] University Centre in Svalbard (UNIS), Longyearbyen, Norway

ABSTRACT

Second order diffraction effects often occur in hyperspectral instruments with dispersive elements. These second (and higher) order diffractions are typically unwanted, and should therefore be removed. One way of achieving this is by using a filter to block parts of the spectrum, calculate the second order light efficiency, and further use this to remove the estimated second order light in all datasets. Here, data from four different filters (two longpass and two shortpass) with three different types of illumination (a radiometric calibration source, cloudy sky and sunny sky) are compared. The shortpass filters used with the sunny sky give best results, while the longpass filters prove useful for validation purposes. A natural light source such as the Sun is shown to be beneficial compared to the calibration source (low intensity in UV) due to differences in spectra from real life measurements.

Index Terms— Hyperspectral imager, second order diffraction effects, second order correction

1. INTRODUCTION

The use of Hyperspectral Imagers (HSIs), or imaging spectrometers, in both industrial and scientific projects is growing. In addition to large, expensive and high-end instruments, small and low-cost instruments built in-house are being developed, e.g. [1, 2, 3]. Smaller and cheaper instruments are more prone to error sources due to the use of cheaper components and less tailored and complex designs. They are, however, useful for many applications and enable more widespread use of HSIs. Simple methods to improve the collected datasets from these imagers are therefore desirable and useful for the community.

The dispersion of light from a diffraction grating can be described by the grating equation

$$k\lambda = d(\sin\alpha + \sin\beta), \tag{1}$$

where k is the spectral order, λ is the wavelength, d is the grating groove spacing, α is the angle of the incoming light (incident angle) and β is the angle of the diffracted light (diffraction angle) [4]. This shows that second order light at wavelength λ_1 is diffracted at the same angle as the first order light from λ_2 when $\lambda_2 = 2\lambda_1$. For a diffraction grating, the relationship between the overlapping orders of light is linear (as opposed to grism designs which can have a nonlinear relationship) and follows the relation

$$\lambda_k = \frac{(k+1)\lambda_{k+1}}{k}, \tag{2}$$

where k again denotes the order of the diffracted light so that λ_k is a wavelength at one order lower than λ_{k+1} that reach the same area on the detector [5]. It is desirable to develop a method to remove the second order light present in the upper part of the spectrum so that these longer wavelengths can be used for analysis, thereby expanding the usable range of instruments limited by these higher order diffraction effects.

One way to measure second order light is by using filters as presented in [5] and [6]. The relationship between the first and second orders of light is found by comparing measurements acquired with and without a filter. This is further used for correction by simply subtracting the estimated amount of second order light from the longer wavelengths based on the amount of incoming first order light. The method presented here is based on this approach. Estimating the second order light using only the intensity differences as done with these filter measurements, however, makes the correction sensitive to differences in the incoming light spectrum. For the diffracted second order light the light spreads out, which both decreases the intensity (peak height) and increases the Full Width at Half Maximum (FWHM) (peak width). A significant change in the incoming spectrum can therefore result in a less accurate correction since overlapping signal from neighboring wavelengths changes, which is not captured by the filter measurements.

Other methods that can be used include measuring second order light with a monochromator, and using in-flight measurements. With a monochromator, changes in both intensity and FWHM can be measured, thereby avoiding the weakness of the filter method. Interpolation can then be used to cre-

The Research Council of Norway is acknowledged for funding through AMOS (grant number 223254) and the IKTPLUSS project MASSIVE (grant number 270959), and the Norwegian Space Agency and the European Space Agency acknowledged for funding through PRODEX (no. 4000132515).

ate a more extensive model of the instrument, as presented in [7]. A full spectral stray light correction of the instrument can also be made, as presented in [8]. This does, however, require a more complex set-up.

In-flight data can also be used. In [9], in-flight ocean data with underwater features such as coral reefs is used to characterize the amount of second order light in the data. Since solar radiation at longer wavelengths (800 nm and above) are absorbed by the water, coral reef features present at the longer wavelengths are from second order light. This is used to quantify the second order effects and correct data during flight. [10] uses a similar method, combining the in-flight and filter method by using different reflectance standards on ground. A compensation model to correct a Ultraviolet (UV)-Visible (VIS) instrument is presented using different colored tiles (UV included and UV excluded standards) to predict the relationship between the first and second order signals. The second order light in the other datasets are then corrected based on the amount of incoming first order light, as for the filter method. Using these standards also includes some atmospheric effects which can be useful for remote sensing instruments. The weakness of dependence on incoming light spectrum is, however, still present.

Here, the filter method approach is used. A filter is attached in front of the HSI to measure the amount of second order light, and the second order light efficiency (ratio of second order light to first order light) is found. This is further used for correction by removing the estimated amount of second order light (based on the incoming first order light) in the data. Four different filters and three different illumination sources are used to investigate which filters and light sources that are most useful for this method. The amount of second order light is measured, and the second order efficiencies and resulting corrections are compared.

2. METHODS

The hyperspectral imager used in this report is a pushbroom HSI based on Commercial Off-The-Shelf (COTS) components with a transmission grating design, as presented in [2]. The designed spectral range is 400 to 800 nm. However, the full sensor covers about 240 to 970 nm. Little light is recorded below 400 nm due to low Quantum Efficiency (QE) of the sensor and absorption by the glass lenses. Second order diffraction effects from the wavelengths at 380 nm and up are, however, expected to appear from about 760-800 nm and upwards, contaminating the spectrum. Specifications of the instrument are summarized in Table 1.

Four filters from Edmund Optics (EO) are used. There are two Longpass (LP) filters with cut-on wavelengths at 500 nm (EO #15-224) and 525 nm (EO #64-626), and two Shortpass (SP) filters with cut-off wavelengths at 700 nm (EO #15-261) and 750 nm (EO #15-262). The LP filters block the light below the cut-on wavelength, and will only record first order light above 780 nm. The SP filters, on the other hand, block the light above the cut-off wavelength. All light recorded above the cut-off wavelength is therefore second order light. The light sources used are a radiometric calibration lamp in an integrating sphere (Model ISS-30VA, Gigahertz Optik), and natural light from the Sun on a cloudy and sunny day.

Table 1: Specifications of the HSI.

Parameter	Specification
Camera sensor	Sony IMX174
Image size	(1936, 1216) pixels
Designed spectral range	400 - 800 nm
Theoretical FWHM	3.3 nm
Spectral sampling distance	0.38 nm per pixel
Grating	300 lines/mm, transmission
Slit height	7 mm
Slit width	50 μm

2.1. Data acquisition

When acquiring data, each of the filters were attached to the front lens of the HSI in turn (order LP 500 nm, LP 525 nm, SP 700 nm, SP 750 nm), and pointed towards the light source. In total, 12 datasets were captured (four filters in combination with each of the three light sources). In addition, a measurement without the filter attached was taken between each measurement to monitor fluctuations in the light level. An extra dataset was also acquired for the purpose of testing the corrections on an independent dataset. For each dataset, 10 images were taken and averaged to reduce noise. Further, only the center line (center of the slit image) was investigated to avoid smile effects. The method can be expanded to the full image by either using smile corrected data or repeat the analysis for each line in the image.

2.2. Data processing

First, the datasets collected in front of the radiometric calibration source were used to calculate the transmission curves of the filters. Reference curves from EO are available, as shown in Figure 1, but these are for the general filter, and not for each specific filter. Minor differences may therefore occur. The cut-on and cut-off wavelengths were found to coincide nicely with the reference curves, while the exact transmission of other wavelengths deviated slightly. The measured curves were therefore used further as filter efficiency curves. In addition, the transmission peak visible for the SP 700 nm filter was removed.

Next, the fluctuation of the light level was investigated by looking at the datasets collected without filters attached. The collected data is shown in Figure 2. The radiometric calibration source and the sunny sky were found to be stable. The cloudy sky, however, fluctuated a lot in light level,

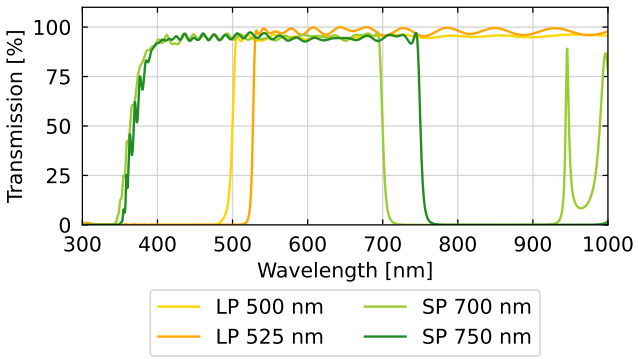

Fig. 1: Filter efficiency curves (from Edmund Optics) for the longpass (LP) and shortpass (SP) filters.

even though the data was captured within a time frame of 10 minutes. For these measurements, a scaling factor was therefore manually found and applied to the cloud measurements to achieve the same signal strength before the data was used further. From this data, it can also be seen that the spectra are slightly different for each light source. The peak is around 600 nm for the calibration source, and closer to 500 nm for the natural light. In addition, features such as Fraunhofer lines are visible in datasets using the Sun as light source.

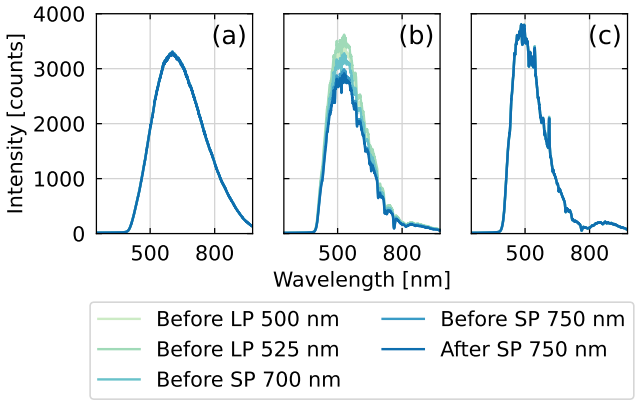

Fig. 2: Measurements without filter, to observe variations in the light level. (a) Radiometric calibration source, (b) cloudy sky, (c) blue sky.

The images captured with filters were normalized by dividing by the corresponding filter efficiency curves. For the SP filters, data above the cut-off wavelength was kept untouched, as this signal is from the second order effects that are being investigated. The resulting filter measurements are shown in Figure 3. The lines coincides well, except for the areas where the filter blocks the light, which is as expected. However, above 750 nm the signals slightly disperse. This is due to the second order light.

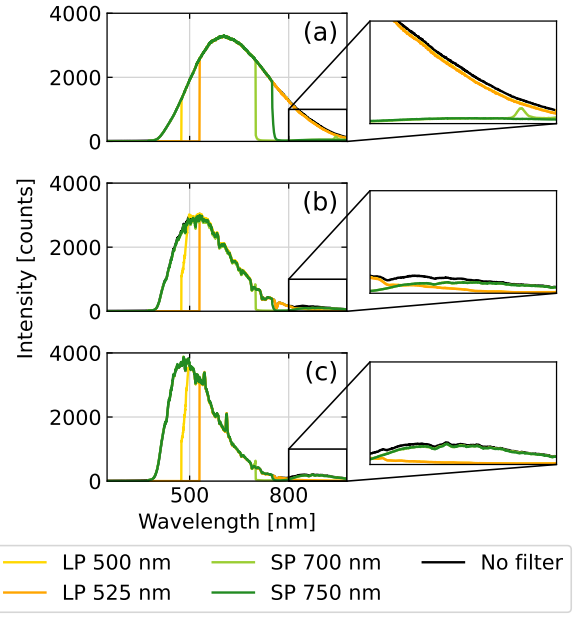

Fig. 3: The normalized datasets. (a) Radiometric calibration source, (b) cloudy sky (scaled), (c) blue sky.

3. SECOND ORDER EFFICIENCY

Using the two different types of filters gives two independent ways of measuring the same second order light. With the LP filters the second order light can be estimated by subtracting the first order light from the total signal (first and second order together which is present in the no filter data). With the SP filters the second order light is measured directly. The estimated amount of second order light is shown in Figure 4a-c. For the radiometric calibration source data (Figure 4a) very little second order light in the 800 to 900 nm range is present due to little light below 450 nm from the calibration source (as seen in Figure 3a). The second order light found here, specially with the LP filters, is therefore very noisy. The peak from the SP 700 nm filter efficiency curve is also visible here due to strong intensity in the radiometric source at shorter wavelengths. This suggests that this filter should not be used when measuring the second order effects above 930 nm. For the cloudy and sunny sky data, however, the second order light measured by the SP filters and estimated with the LP filters coincides well. It can also be noted that the LP data has lower and more noisy signal below 800 nm than the SP filter data.

From the estimated second order light, the second order light efficiency, A_λ, was calculated. This describes the amount of second order light that is produced by the different first order wavelengths, and is calculated as

$$A_\lambda = \frac{C_{\lambda\ \text{(second order)}}}{C_{\lambda/2\ \text{(first order)}}}, \tag{3}$$

where $C_{\lambda\ \text{(second order)}}$ is the second order signal appearing at

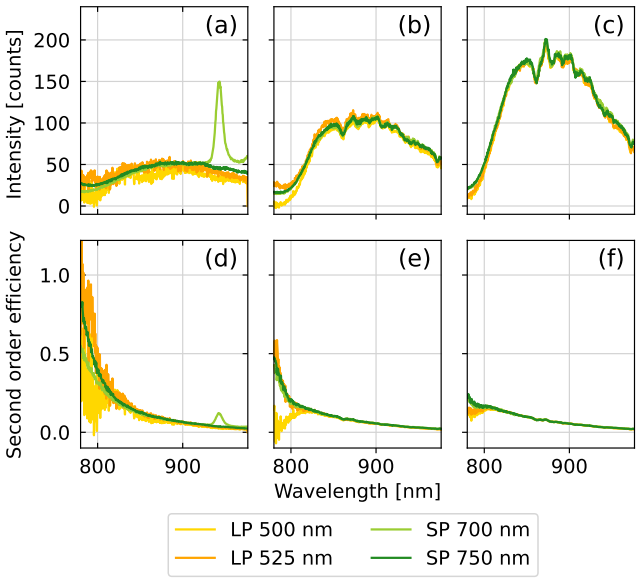

Fig. 4: Estimated second order light (a-c) and calculated second order light efficiency (d-f) for the three data sets with all four filters. (a,d) Radiometric calibration source, (b,e) cloudy sky, (c,f) blue sky.

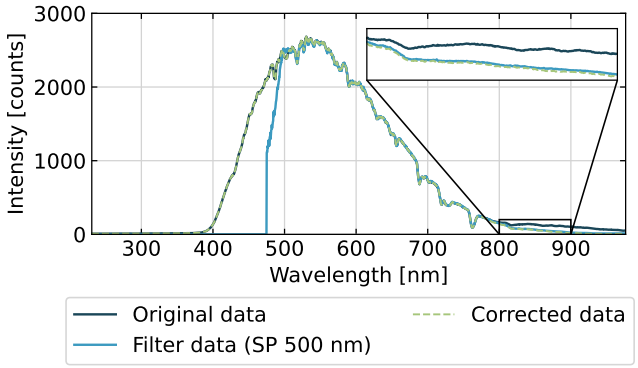

Fig. 5: Example of second order correction by filter (here using the SP 750 nm filter). Additional filter data is shown as reference of data without second order light. Zoomed in inlet shows that the corrected signal (dashed) follows the reference signal nicely.

a given wavelength λ, while $C_{\lambda/2\,\text{(first order)}}$ is the first order signal of the same wavelength.

The calculated second order light efficiency for all three data sets with all four filters are shown in Figure 4d-f. It can be seen that the LP data is generally noisier than data from the SP filter, especially below 800 nm. This is as expected when looking at the second order light in Figure 3, as they have lower intensities below 800 nm. It can also be seen that the estimated second order efficiency diverges below approximately 810 nm. This is mostly due to the first order signal from around 400 nm having very low signal strength with relatively high levels of noise. The results in this region are therefore expected to be less accurate. Above 850 nm, however, the curves have similar values both across filter types and light sources, suggesting that these values are more reliable. Again, it can be noted that the peak from the SP 700 nm filter is visible in the radiometric calibration source plot, which is an artifact of the filter and not the correct second order efficiency.

The curves were smoothed by a Bartlett window to reduce noise before they were used further for corrections.

4. SECOND ORDER CORRECTION

Correction can then be achieved by applying

$$C_{\lambda,\,\text{corr}} = C_\lambda - C_{\lambda/2} A_\lambda, \tag{4}$$

where $C_{\lambda,\,\text{corr}}$ is the corrected signal at wavelength λ (for example signal at 800 nm, without any second order light present), C_λ represents the number of measured counts at this first order higher wavelength (the signal recorded at 800 nm before correction), $C_{\lambda/2}$ is the number of measured counts at the corresponding second order lower wavelength (the measured light at 400 nm), and A_λ is the calculated efficiency describing the amount of generated second order light expected to occur at the higher wavelength based on the amount of first order signal (the amount of second order light from 400 nm appearing at 800 nm).

An example of how the correction works on the test data is shown in Figure 5 (corrected with the second order efficiency from the sunny sky dataset with the SP 750 nm filter). Filter data (LP 500 nm) from the test dataset is also shown for reference. The goal is that the corrected signal follows the original signal until the second order effects appear, and then follows the filter data where the second order effects are filtered out. The figure shows that the corrected signal behaves as expected.

The correction applied to the same test dataset using all calculated second order light efficiencies (four filters, three light sources) are shown in Figure 6. It can be seen that the correction based on the radiometric calibration dataset performs worst, as the corrected signals deviate from the reference filter data. This is most likely due to the low amounts of second order light in the original dataset, with high levels of noise, resulting in a poorer estimate of the second order efficiency. And again, the peak from the SP 700 nm filter can be seen, this time as a dip at 930 nm after the correction with values close to negative 150 counts. This shows that filter artifacts can greatly disturb the correction, and filters with such peaks and dips in their transmission curves should not be used. The corrections based on the datasets when observing the sky, however, shows better performance. They both estimate a bit too much second order light, resulting in slightly lower signal after correction than what the reference filter data

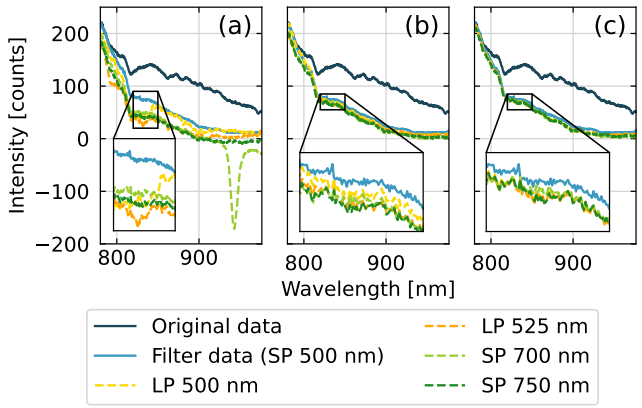

Fig. 6: Second order correction applied to the test data, using the second order efficiency calculated by all four filters with all three light sources. (a) Radiometric calibration source, (b) cloudy sky, (c) blue sky.

shows. The cloudy sky dataset gives on average a signal that is 14% below the reference, while the blue sky data is on average 11% below the filter reference data. Even though the test dataset is also looking at a cloudy sky, the correction based on the blue sky datasets performs better, suggesting that a stable light source is beneficial when collecting the filter data measurements.

5. CONCLUSIONS AND FUTURE WORK

From these experiments, we have shown that correction of second order light can be achieved by calculating the second order efficiency from data collected with filters, and use this to remove second order light in the dataset. The SP filters measure the second order light spectrum directly, and is therefore the easiest to use. The LP filters are useful for validation purposes as they only record first order light at the longer wavelengths, which can be used as a reference for correct signal at these wavelengths. It is important to choose filters without artifacts such as steep peaks and dips in the filter curves (unless these are accounted for properly), as these affects the calculation of the second order efficiency and thereby the correction results.

For a light source, it is preferable with a stable light source (or target), and a spectrum which is close to what will be used during operations. The Sun/natural light is therefore a good choice for remote sensing instruments that will be used outdoors with the Sun as illumination. It is also nice to keep in mind that a higher Signal-to-Noise Ratio (SNR) is beneficial when performing the measurements, as the second order effects are typically quite weak in intensity and therefore becomes noisy if the signal strength is not high enough.

For future work, comparing the correction based on filters with corrections from monochromator measurements ([7, 8]) and in-flight data ([9, 10]) would be a useful addition to assess which method should be used. A more detailed analysis of the accuracy of the corrections should also be done.

6. REFERENCES

[1] F. Sigernes, M. Syrjäsuo, R. Storvold, J. Fortuna, M. E. Grøtte, and T. A. Johansen, "Do it yourself hyperspectral imager for handheld to airborne operations," *Optics Express*, vol. 26, no. 5, pp. 6021–6035, 2018.

[2] M. B. Henriksen, E. F. Prentice, C. M. van Hazendonk, F. Sigernes, and T. A. Johansen, "Do-it-yourself VIS/NIR pushbroom hyperspectral imager with C-mount optics," *Optics Continuum*, vol. 1, no. 2, pp. 427, 2022.

[3] H. Saari, V. Aallos, A. Akujärvi, T. Antila, C. Holmlund, U. Kantojärvi, J. Mäkynen, and J. Ollila, "Novel miniaturized hyperspectral sensor for UAV and space applications," in *Proc. SPIE 7474, Sensors, Systems, and Next-Generation Satellites XIII, 74741M*, 2009.

[4] C. Palmer and E. Loewen, *Diffraction Grating Handbook*, Newport Corporation, 7 edition, 2014.

[5] V. Stanishev, "Correcting second-order contamination in low-resolution spectra," *Astronomische Nachrichten*, vol. 328, no. 9, pp. 948–952, 2007.

[6] W. Lee, H. Lee, and J. W. Hahn, "Correction of spectral deformation by second-order diffraction overlap in a mid-infrared range grating spectrometer using a PbSe array detector," *Infrared Physics and Technology*, vol. 67, pp. 327–332, 2014.

[7] S. I. Bruchkouskaya, G. S. Litvinovich, I. I. Bruchkousky, and L. V. Katkovsky, "Algorithm for second-order diffraction correction in a concave diffraction grating spectrometer," *Journal of Applied Spectroscopy*, vol. 86, no. 4, pp. 671–677, 2019.

[8] Y. Zong, S. W. Brown, B. C. Johnson, K. R. Lykke, and Y. Ohno, "Simple spectral stray light correction method for array spectroradiometers," *Applied Optics*, vol. 45, no. 6, pp. 1111–1119, 2006.

[9] R. R. Li, R. Lucke, D. Korwan, and B. C. Gao, "A technique for removing second-order light effects from hyperspectral imaging data," *IEEE Transactions on Geoscience and Remote Sensing*, vol. 50, no. 3, pp. 824–830, 2012.

[10] Z. Xu and M. H. Brill, "Correction of second-order-diffraction errors in spectrophotometry," *Color Research and Application*, vol. 42, no. 2, pp. 189–192, 2017.